

High strain rate compressive behavior of PMMA

S. Acharya · A. K. Mukhopadhyay

Received: 15 January 2013 / Revised: 7 May 2013 / Accepted: 27 August 2013 /
Published online: 4 September 2013
© Springer-Verlag Berlin Heidelberg 2013

Abstract Polymethylmethacrylate (PMMA) materials are extensively used for diverse applications e.g., protective vehicular windows to eye protection devices. However, the high strain rate deformation and fracture mechanisms of PMMA are far from well understood. Therefore, controlled split Hopkinson pressure bar (SHPB) experiments that could lead to deformation with and without fracture were conducted on PMMA samples at strain rates of $\sim 4 \times 10^0$ to $1.3 \times 10^3 \text{ s}^{-1}$. With increase in strain rate, the maximum compressive yield strength of PMMA is enhanced by about 25 %. Absence of global failure characterized the deformation at relatively lower strain rates (e.g., $\sim 4.75 \times 10^2$ to $6.75 \times 10^2 \text{ s}^{-1}$), while its marked presence characterized the same at comparatively higher strain rates (e.g., $\sim 7.69 \times 10^2$ to $9.31 \times 10^2 \text{ s}^{-1}$). Attempts were made to explain these observations by the subtle changes in failure mechanisms as revealed from the fractographic examinations of the PMMA samples deformed with and without failures. The implications of the test-condition induced restrictions on the degrees of freedom locally available to the polymeric chains were discussed in the perspective of the relative strain rate dependencies of the yield behaviors of the present PMMA samples.

Keywords Polymer · PMMA · Strain rate · Dynamic · Behavior

S. Acharya (✉)
Non-Oxide Ceramic and Composite Division, CSIR-Central Glass and Ceramic Research Institute,
Kolkata 700032, India
e-mail: saikat@cgcri.res.in

A. K. Mukhopadhyay
Mechanical Property Evaluation Section, Material Characterization Division, CSIR-Central Glass
and Ceramic Research Institute, Kolkata 700032, India

Introduction

Polymethylmethacrylate (PMMA) is widely used as a protective structural material in many applications e.g., aerospace, automobile, and strategic sectors. To ensure reliable performance of PMMA it is therefore essential to understand the deformation and failure mechanisms of it. Therefore, a lot of past and present research activities [1–14] have been carried out to develop better understanding about the deformation and failure mechanisms of PMMA. The need for the development of such understanding becomes particularly more important for high impact shock stress resistant applications, which involve high strain rates.

Many researchers [1–14] have devoted attention to the yield behavior of PMMA as a function of the variations in strain rates and temperatures. For instance, Roetling [1] studied the yield strength of PMMA as a function of strain rate and temperature, and indicated a strain rate-dependent transition of the yield behavior. Similarly, Moy et al. [2] found that failure of PMMA was strain rate sensitive in both quasi-static and dynamic loading. Further, the stress–strain response was reported to exhibit a decrease in the flow stress with an increase in temperature. On the other hand, Richeton et al. [3, 4] reported that both temperature and strain rate could significantly affect the yield behavior of PMMA. Wu et al. [5] observed that when the strain rate is increased, the strength and initial modulus of PMMA are enhanced, while the strain suffered at fracture gets degraded. Similar observations were also reported by Chen et al. [6]. These researchers noted that PMMA displays smaller failure strains under high strain rate uniaxial dynamic tension, but exhibits significantly higher compressive strength under high strain rate uniaxial compression conditions.

On the other hand, Li et al. [7, 8] claimed that the compressive yield stress of PMMA increased with the increase of strain rate. They further noted that as strain rate is enhanced subsequently, the material could change its compressive failure behavior from ductile to brittle. However, some heating was also observed during the failure of the PMMA specimen suggesting that at such high strain rates (e.g., $\sim 10^{-4}$ to 10^3 s $^{-1}$) the material was not perfectly brittle. Blumenthal et al. [8] reported that the strength of PMMA was linearly dependent on temperature and strongly sensitive to variations in the strain rates. In addition, it was observed that it developed cracks and failed in compression with exhibition of only a little ductility at either low strain rates and low temperatures or at high strain rates and temperatures very close to those of the ambient. Therefore, it would appear that there is an apparent contradiction between the observations reported in references [7] and [8].

It is most interesting to note that when strain rate responses of PMMA were investigated under uniaxial compression at different rates of strain, Moy et al. [9] noted that at strain rates of ≤ 1 s $^{-1}$, the intrinsic softening that occurred after the initial yield, was followed by strain hardening. It was found further [9] that at a critical strain rate of 1 s $^{-1}$, the material started to soften further due to the dominance of thermal softening over strain hardening. However, at strain rates of greater than 1 s $^{-1}$, PMMA failed before, during or immediately after the yield, depending on the rate of loading.

Chou et al. [10] measured the rise of temperature during deformation of PMMA using a thermocouple. The experimental results reported by them showed a positive viscous effect at the beginning of the deformation, followed by plastic flow. Walley et al. [11] observed that the strain hardening behavior of the glassy polymers was dependent on both strain rates and temperatures.

Arruda et al. [12] found that even at moderate (e.g., 10^{-2} and -10^{-1} s $^{-1}$) strain rates, PMMA exhibited post-yield softening. Similarly, Swallowe et al. [13, 14] reported that deformation of various polymers at high strain rates (e.g., from $\sim 10^{-4}$ to 10^3 s $^{-1}$) converted mechanical energy partially into heat energy in the immediate vicinity of the crack tips. It was suggested further that [13, 14] such an energy conversion process could have had happened on either locally available shear planes or uniformly throughout the bulk. In addition, it was further observed [13, 14] that β -relaxation along with α -relaxation could occur when the strain rate had surpassed the critical value of 1 s $^{-1}$.

It is evident from the shear existence of so many viewpoints and observations as enunciated above, that in spite of the wealth of literature, the mechanisms involved in high strain rate compressive deformation and failure of PMMA are yet to be unequivocally established. Therefore, the objective of the present study was to conduct split Hopkinson pressure bar (SHPB) experiments on PMMA at relatively high strain rates (e.g., $\sim 4 \times 10^0$ to 1.3×10^3 s $^{-1}$), with a view to develop better understanding about the compressive deformation and failure mechanisms of the same. It was decided to conduct the experiments under controlled applied stresses in such a fashion so as to cause deformation with and without fracture to occur in the present PMMA samples such that the issues of failure mechanisms at high strain rates can be better resolved.

Materials and methods

Commercially available PMMA (Anulon-120, M/S Plastic Abhiyanta, Kolkata, India) samples were used. The data on the physico-mechanical properties of the particular grade of PMMA as quoted by the supplier are given in Table 1.

Table 1 Physico-mechanical properties of PMMA samples

Property	Standard	Value
Density	DIN 53479	1.18 g/cm 3
Softening temperature	DIN 53460	102 °C
Coefficient of linear thermal expansion	VDEO 304/1	70–10 $^{-60}$ C $^{-1}$
Thermal conductivity	DIN 52612	0.19 W/m 0 C
Impact strength	DIN 53453	12 kJ/m 2
Tensile strength	DIN 53455	72 MPa
Elongation at break	DIN 53455	4.5 %
Flexural strength	DIN 53452	105 MPa
Compressive yield stress	DIN 53454	103 MPa
Modulus of elasticity	DIN 53457	3,300 MPa

It has been reported that cylindrical polymer specimens with thickness (l_s) to diameter (d) ratio (l_s/d) of 0.5–2.0 are appropriate for compressive SHPB testing [15]. The diameter (d) and thickness (l_s) of the PMMA specimens used in the present experiments were kept in the range of 10.09 ± 0.04 and 5.09 ± 0.04 mm, so that the slenderness ratio (l_s/d) was about 0.5 to ensure stress equilibrium [16–18].

Four different sets e.g., A, B, C, and D of the PMMA samples were used in the present experiments. Each of these sets contained four samples e.g., the data represented as that of sample A is the average data measured for the samples A1, A2, A3, and A4. The similar situations were true for the samples B, C, and D. But for the sake of brevity, clarity and comparative discussion only the average, representative data are presented here for the four sets of PMMA samples e.g., A, B, C, and D. The loading was controlled in such a fashion that the PMMA samples A and B had undergone deformation followed by fracture, whereas the PMMA samples C and D had undergone deformation without fracture.

In the current SHPB experiments, the pulse-shaping technique was used. As suggested by other researchers [6, 19], the application of this technique ensures stress equilibrium in the specimen during the dynamic compression experiments conducted at high strain rates. Thus, tiny copper pulse shapers of ~ 5 mm diameter and ~ 0.5 mm thickness were used in the experiments.

The PMMA samples were typically kept as sandwiched between the incident bar and the transmitter bar and loaded in dynamic compression. One pair of strain gauges was mounted exactly at the mid-length positions on both incident and transmitter bars. The strain rate and stress data were obtained from the reflected strain (ε_R) and transmitted strain (ε_T) pulses received from the gauges mounted on the incident and transmitter bars, respectively.

The following Eqs. e.g., (1), (2), and (3) from References [19, 20] were used to calculate the strain rate $\dot{\varepsilon}_s(t)$, the average strain $\varepsilon_s(t)$, and the maximum compressive yield stress $\sigma_{Yc}(t)$ of the PMMA specimens used in the compressive SHPB testing:

The strain rate,

$$\dot{\varepsilon}_s(t) = (2C_0/l_s)\varepsilon_R(t) \quad (1)$$

The average strain,

$$\varepsilon_s(t) = \pm(2C_0/l_s) \int_0^t \varepsilon_R(t) dt \quad (2)$$

The maximum compressive yield stress,

$$\sigma_{Yc}(t) = \pm E \frac{A_B}{A_s} \varepsilon_T(t) \quad (3)$$

Here, C_0 is elastic wave velocity in the bars, l_s is specimen length, A_s is the cross-sectional area of the specimen, A_B is the cross-sectional area of the bar, E is Young's modulus of the bar, and t is time.

As mentioned earlier, the compressive stress–strain responses of the four different sets A, B, C, and D of PMMA were measured in the present work under two different experimental conditions. In the first case, the high strain rate compressive responses were measured when the PMMA specimens A and B had

undergone deformation followed by fracture. In the second case, however, the same were measured when the PMMA specimens C and D had undergone deformation without fracture.

Results and discussions

The experimental data on force versus time are presented in Fig. 1. It may be noted that the dynamic equilibrium of the related forces requires that the sum ($F_I + F_R$) equals F_T , where F_I is the incident, F_R is the reflected and F_T is the transmitted component of force (F). Under ideal conditions when there is cent percent proper surface-to-surface contact between the incident and transmitter bars, F_R should be zero and the dynamic equilibrium of the forces requires that the force component F_I equals the force component F_T . In real contacts, however, F_R is non-zero. The strain data were recorded from the pair of strain gauges mounted on the incident bar. The values of Young's modulus (e.g., $E \sim 200$ GPa) and cross-sectional area (e.g., diameter ~ 20 mm) of the incident bar made up of hardened steel were utilized to calculate the magnitudes of $F_I + F_R$. Similarly, the relevant data were used for the transmitter bar to calculate the magnitude of F_T . The typical calibration data plot (Fig. 1) obtained from the SHPB experiments presented without the sample sandwiched between the incident and transmitter bars showed that the two force curves mostly overlapped with each other signifying that the stress conditions in the incident and transmitter bars were closely analogous. It also confirmed that the dynamic force equilibrium was achieved in the present experiments. Therefore, it may be concluded that the SHPB apparatus used in the present experiments was properly calibrated, aligned and reasonably friction free.

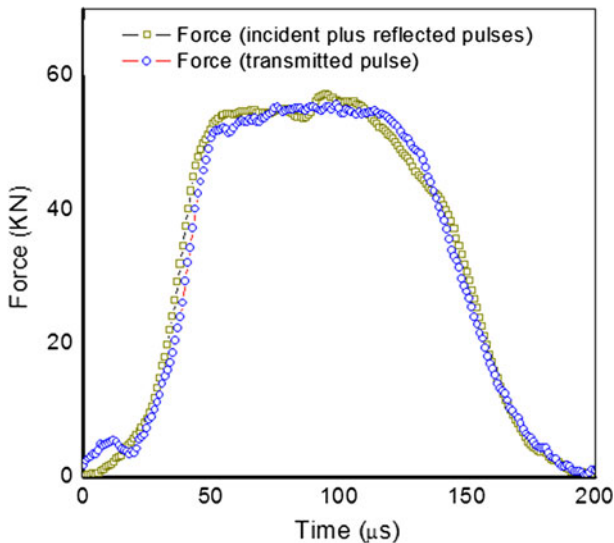


Fig. 1 Typical force versus time data plot for the incident, reflected and transmitted pulses obtained from the SHPB experiments

In the case of the sample C, the data presented in Fig. 2a showed that the combined duration (e.g., 275 μs) of the reflected and transmitted strain pulses was longer by about 69 μs than that (e.g., 206 μs) of the incident strain pulse. Similarly, the data presented in Fig. 2b for specimen D, established that the combined duration (e.g., 265 μs) of the reflected and transmitted strain pulses was longer by about 45 μs than that (e.g., 220 μs) of the incident strain pulse.

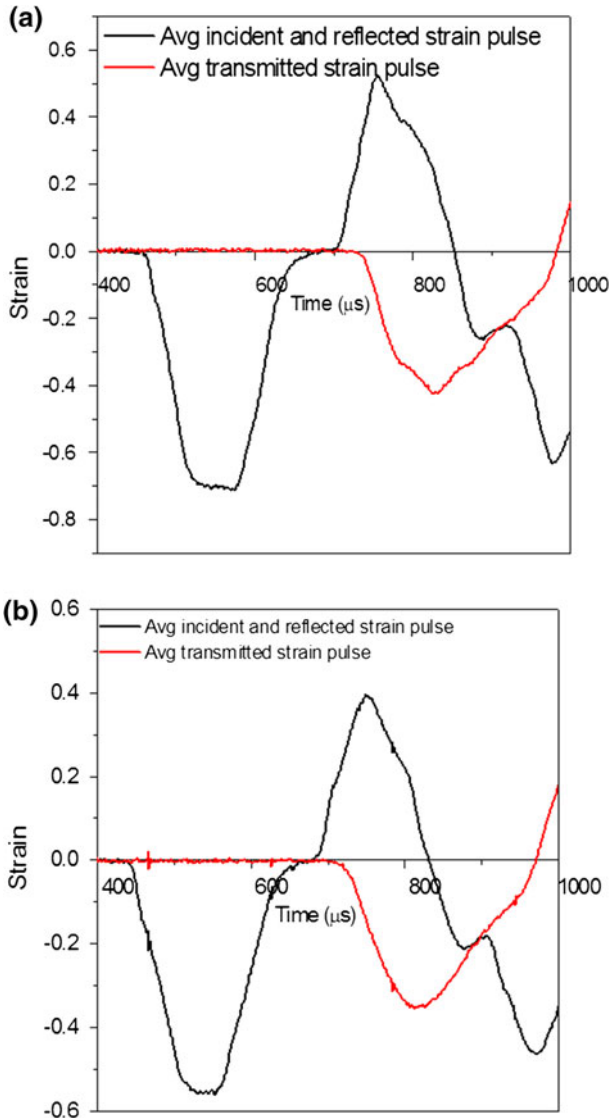


Fig. 2 Typical dynamic incident, reflected, and transmitted strain pulses obtained from the SHPB experiments conducted on the PMMA samples: **a** C and **b** D

When the compressive incident strain pulse reaches the interface between the PMMA sample and the transmitter bar, a part of it gets reflected back from the interface into the sample, while the rest part gets transmitted into the transmitter bar as mentioned above. It is plausible to imagine that at any given instant there could be many strain pulses generated inside the PMMA sample due to the first incident compressive strain pulse. When one such strain pulse will have a part transmitted through the transmitter bar and a part reflected back into the sample from the interface, it becomes highly likely as well that this reflected back strain pulse could get itself overlapped with the most immediate next strain pulse that is trying to pass through the PMMA sample towards the interface. This is most likely why the specimen took longer time to recover up to zero stress during unloading. A comparison of the data plotted in Fig. 2a, b would suggest that the compressive stress endurance of sample C (unbroken at strain rate $\sim 1.02 \times 10^3 \text{ s}^{-1}$) would be slightly higher than that of sample D (unbroken at strain rate $\sim 7.81 \times 10^2 \text{ s}^{-1}$).

For the PMMA sample types A, B, C, and D, the typical average, representative data on strain rate and stress versus time have been plotted in Fig. 3. These data showed many characteristic features of the deformation and failure processes which shall be discussed now.

The data presented in Fig. 3 indicated that four PMMA samples “A”, “B”, “C”, and “D” had respectively achieved maximum strain rates of $\sim 1.34 \times 10^3 \text{ s}^{-1}$ at $\sim 52 \mu\text{s}$ at the point marked as A, $\sim 1.19 \times 10^3 \text{ s}^{-1}$ at $\sim 62 \mu\text{s}$ at the point marked as B, $\sim 1.02 \times 10^3 \text{ s}^{-1}$ at $\sim 55 \mu\text{s}$ at the point marked as C, and $\sim 7.81 \times 10^2 \text{ s}^{-1}$ at $\sim 69 \mu\text{s}$ at the point marked as D. The point marked as F_A in Fig. 3 indicated the region where sample type “A” had fractured at a strain rate of e.g., $\sim 9.31 \times 10^2 \text{ s}^{-1}$ at $\sim 87 \mu\text{s}$. Similarly, the point marked as F_B in Fig. 3 indicated

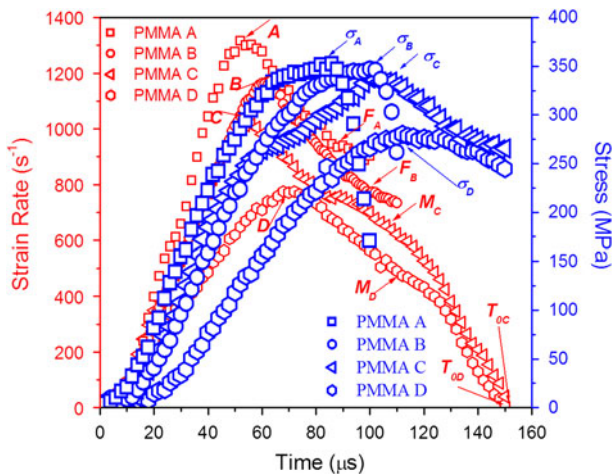


Fig. 3 The typical, representative, average strain rate, and the corresponding stress data obtained as a function of time as measured from the SHPB experiments conducted on the PMMA samples A, B, C, and D

the region where sample type “B” had fractured at a strain rate of e.g., $\sim 7.69 \times 10^2 \text{ s}^{-1}$ at $\sim 101 \mu\text{s}$.

However, the point marked M_C indicated the region where sample “C” had endured the maximum compressive stress at a strain rate of e.g., $\sim 6.75 \times 10^2 \text{ s}^{-1}$ at $\sim 101 \mu\text{s}$. Thus, the point marked M_D indicated the region where the sample “D” had endured the maximum compressive stress at a strain rate of e.g., $\sim 4.75 \times 10^2 \text{ s}^{-1}$ at $\sim 112 \mu\text{s}$.

Further, the points marked as T_{0C} and T_{0D} indicated the regions, where the samples “C” and “D” returned to their almost “near-zero” compressive stress states at strain rates of e.g., $\sim 0.70 \text{ s}^{-1}$ at $\sim 152 \mu\text{s}$ and $\sim (-4.84 \text{ s}^{-1})$ at $\sim 151 \mu\text{s}$, respectively. The “-” sign suggested that possibly the stress state had changed from a compressive one to a tensile one.

The data on stress versus time (Fig. 3) indicated that the PMMA samples “A” and “B” had achieved respectively the maximum compressive yield stresses of $\sim 351 \text{ MPa}$ at the point marked as σ_A at e.g., $\sim 87 \mu\text{s}$ and $\sim 345 \text{ MPa}$ at the point marked as σ_B at e.g., $\sim 101 \mu\text{s}$. As mentioned earlier, both of these samples had suffered catastrophic failures during the present SHPB experiments.

After analysing the data on stress versus time and strain rate versus time (Fig. 3), it showed that PMMA sample “A” failed when it attended the maximum compressive yield strength (σ_{Yc}) of $\sim 351 \text{ MPa}$ at $\sim 87 \mu\text{s}$ at a strain rate of $\sim 9.31 \times 10^2 \text{ s}^{-1}$ (e.g., at F_A). Corresponding value of maximum compressive yield strength (σ_{Yc}) for sample “B” was $\sim 345 \text{ MPa}$ at $\sim 101 \mu\text{s}$ at a strain rate of $\sim 7.69 \times 10^2 \text{ s}^{-1}$ (e.g., at F_B), when it failed. Thus, the average maximum compressive yield strength (σ_{Yc}) of the PMMA “B” sample was similar to that (e.g., $\sim 351 \text{ MPa}$) of the PMMA sample “A”, as expected.

However, it is also evident from the data presented in Fig. 3 that the PMMA samples “C” and “D” had endured respectively the maximum compressive stresses of $\sim 338 \text{ MPa}$ at the point marked as σ_C at e.g., $\sim 101 \mu\text{s}$ and $\sim 281 \text{ MPa}$ at the point marked as σ_D at e.g., $\sim 112 \mu\text{s}$. Further, the experimental data presented in Fig. 3 confirmed that both of these samples returned to their near-zero compressive stress states.

It is interesting to note that at the point marked as C in Fig. 3, the PMMA sample “C” had attained the typical average the maximum strain rate of $\sim 1.02 \times 10^3 \text{ s}^{-1}$ at a time instant of e.g., $55 \mu\text{s}$. Moreover, the PMMA sample “C” did not fail at this strain rate. Rather, it had continued to endure further stress until it had attained the peak stress e.g., 338 MPa . This region is marked as σ_C in Fig. 3. In addition, this particular point must be emphasized that this magnitude of stress state (e.g., 338 MPa) had been achieved at a much later time instant of e.g., $\sim 101 \mu\text{s}$ (Fig. 3) when the average strain rate was, in fact, a little lower e.g., $\sim 6.75 \times 10^2 \text{ s}^{-1}$. This point is marked as M_C in Fig. 3. The other critical point of importance as revealed by this data was that that beyond this instance of time e.g., $\sim 101 \mu\text{s}$ the sample got slowly unloaded with deformation without fracture as illustrated by a continuous decrease of strain rate with time (Fig. 3).

Finally, after an elapsed time of $152 \mu\text{s}$ i.e., at the point marked as T_{0C} in Fig. 3, the strain rate became zero and subsequently negative (not shown in Fig. 3). The

negative strain rate data may possibly mean that it became tensile from being compressive so long in nature.

It needs to be noted further that at the point marked as *D* in Fig. 3, the PMMA sample “D” had attained the typical average the maximum strain rate of $\sim 7.81 \times 10^2 \text{ s}^{-1}$. This happened after about $69 \mu\text{s}$ taking the instant of impact as the reference zero of the time scale.

Similar to the case of the PMMA sample “C” as discussed above, the PMMA sample “D” also did not fail at this strain rate. Rather, it had continued to endure even higher stress levels until it had attained the peak stress e.g., $\sim 281 \text{ MPa}$. This region is marked as σ_D in Fig. 3. Further, this particular point must be recognized that, this magnitude of stress state had been achieved at a much later time instant of e.g., $\sim 112 \mu\text{s}$ (Fig. 3) when the average strain rate was, in fact, a little lower e.g., $\sim 4.75 \times 10^2 \text{ s}^{-1}$. This point is marked as M_D in Fig. 3. The other critical point of importance was that, beyond this instance of time e.g., $\sim 112 \mu\text{s}$, the sample got gradually unloaded with deformation without fracture as demonstrated by a continuous decrease of strain rate with time (Fig. 3).

In addition, it should be noted further from the data presented in Fig. 3 that finally, after an elapsed time of about $151 \mu\text{s}$ the strain rate became zero and subsequently negative (not shown in Fig. 3). This situation is indicated by the point marked as T_{0D} in Fig. 3. Thus, this data was similar to that (e.g., $152 \mu\text{s}$) of the PMMA sample “C” as discussed above. Here also, the negative strain rate data may possibly suggest that it became tensile in terms of response behavior after having remained as compressive for so long.

Application of the Eq. (2) to the data presented in Fig. 3 also showed that the PMMA sample “A” had failed at a total average typical strain of about 7 % after about $87 \mu\text{s}$ taking the instant of impact as the zero reference data for time. Interestingly, the total average typical strain at failure was also about 7 % for the PMMA sample B; but it had occurred after a little more time (e.g., after $\sim 101 \mu\text{s}$) compared to that ($\sim 87 \mu\text{s}$) of the PMMA sample “A”.

In the case of the PMMA samples “C” and “D”, deformation without fracture was observed. It was reflected in the fact that the strains estimated for PMMA samples “C” and “D” were a little on the lower side. For instance, the application of the Eq. (2) to the data presented in Fig. 3, gave an estimate of about 6.5 % strain attained after about $101 \mu\text{s}$ if the instant of impact is taken as the zero reference data for time. Similarly, in the case of sample “D” the application of the Eq. (2) yields a strain estimate of about 5.5 % achieved after about $112 \mu\text{s}$ had elapsed from the instance of the high strain rate impact event.

Following the method prescribed in reference [21], the typical average representative pictures of the variations of strain rate ($\dot{\epsilon}$) with strain are depicted in Fig. 4a–d for the present PMMA samples e.g., A, B, C, and D. The measured areas under each of these representative curves are as indicated in the insets of Fig. 4a–d. These data actually reflected the amount of energy spent from the compressive loading train per unit volume per unit time by the various PMMA samples during the present SHPB tests. It was further interesting to note that the amount the energy absorbed per unit volume per unit time from the compressive

loading train, by the present PMMA samples, had actually increased with the enhancement of strain rate.

The compressive stress endurance of polymers is highly sensitive to strain rate, which decides the rate at which the energy is transferred from the compressive loading system to the sample. The data presented in Fig. 5 show the comparison of typical, average, representative maximum compressive yield strength, (σ_{YC}) versus average strain rate ($\dot{\epsilon}_{av}$) of PMMA samples used in the present work and the similar data from the works reported by Richeton et al. [4], Li et al. [7], Blumenthal et al. [8], and Mulliken et al. [22].

The data presented in Fig. 5 show that the maximum compressive yield strength, (σ_{YC}) of the present PMMA samples increased with increase of the average strain rate ($\dot{\epsilon}_{av}$). Thus, the present data were similar to the observations reported by a considerable number of earlier researchers [1, 4, 5, 7, 8, 17, 22]. In particular, the inset of Fig. 5 depicts the data (from the present work as well as from literature) which appeared as a cluster as shown by the dotted circle in Fig. 5.

In addition, taking into considerations the data reported in literature [4, 7, 8, 22] and the data from the present work, an empirical power law relationship is predicted

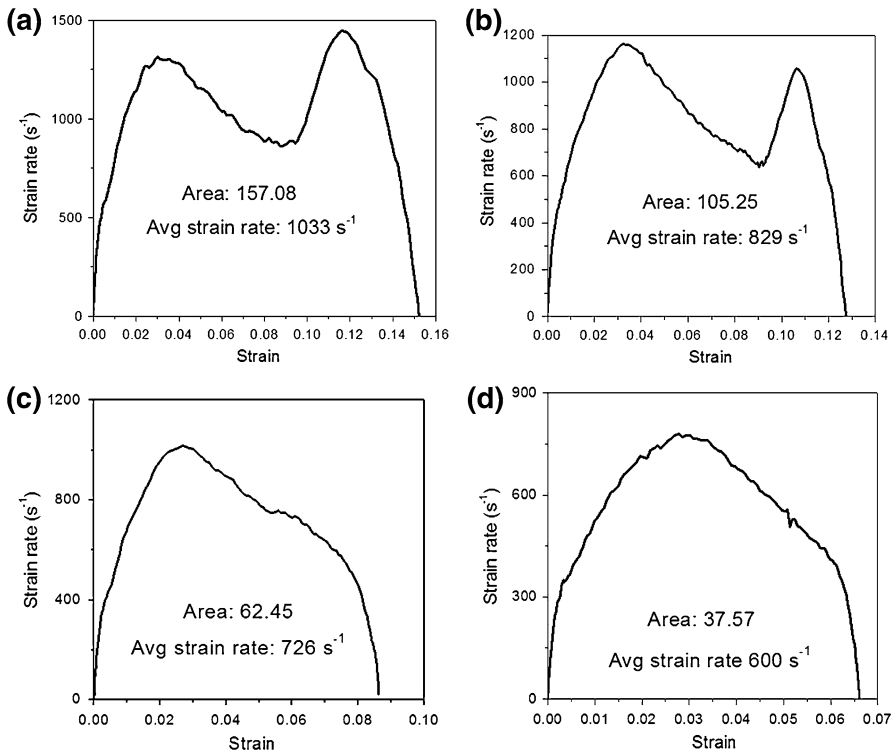


Fig. 4 The typical, representative, average strain rate versus strain data plots as measured from the SHPB experiments conducted on the PMMA samples at various strain rates: **a** PMMA "A" at $1.033 \times 10^3 s^{-1}$, **b** PMMA "B" at $8.29 \times 10^2 s^{-1}$, **c** PMMA "C" at $7.26 \times 10^2 s^{-1}$ and **d** PMMA "D" at $6.00 \times 10^2 s^{-1}$

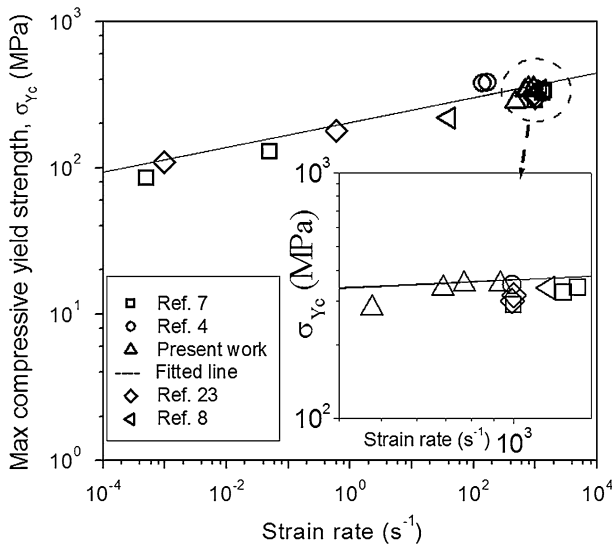


Fig. 5 The maximum average compressive yield strength of PMMA from the present work and literature [4, 7, 8, 22] as a function of the average strain rate. The *inset* shows the details of the portion from the data that appeared to be jumbled up in a cluster

to exist between the maximum compressive yield strength, (σ_{Yc}) and the average strain rate ($\dot{\epsilon}_{av}$). This empirical relationship is described by the following Eq. (4):

$$(\sigma_{Yc}) = 204.17(\dot{\epsilon}_{av})^{0.0848} \tag{4}$$

The empirical relation described by the Eq. (4) proposed in the present work satisfactorily predicts the compressive yield strength of PMMA reported in literature [4, 7, 8, 22], as well as those obtained from the present work. The visual appearance of the predicted trend (Fig. 5) also suggested that the experimental data covering a range of eight orders of magnitudes e.g., from $\sim 10^{-4}$ to 10^4 s^{-1} can be predicted using the relationship proposed by the Eq. (4).

For instance, the present empirical Eq. (4) predicted the maximum compressive yield strength of PMMA as about 95 MPa at a strain rate of 10^{-4} s^{-1} which was within 10 % of the experimental data e.g., 85 MPa measured at the same strain rate of 10^{-4} s^{-1} [7]. Similarly, the proposed empirical Eq. (4) successfully predicted the maximum compressive yield strength of PMMA as about 442 MPa at a strain rate of 10^4 s^{-1} which was within 10 % of the experimental data e.g., about 400 MPa measured at the same strain rate of 10^4 s^{-1} [23].

The close match between the values predicted on the basis of the Eq. (4) proposed in the present work and the experimentally measured data at both very low and very high strain rates reflects upon the efficacy of the empirical relationship. Further, the comparatively lower value of the exponent in Eq. (4) seems to suggest that the extent of strain rate sensitivity of the maximum compressive yield strength for the present PMMA samples might be of comparatively lower magnitude.

In general, the deformation of amorphous polymers e.g., PMMA at high rates of strain can often lead to conversion of the impact energy to heat energy. Whether the

heating would be localized at the crack tip, or on the shear plane, or throughout the bulk of the material would depend on the exact mode of deformation of the PMMA under study [24]. The total energy imparted to the specimen is absorbed either as fracture energy or as elastic strain energy or a combination of the two.

In the cases when the specimen failed e.g., as in the cases of “A” and “B”, the PMMA samples absorbed the total energy from the system. In such cases, the energy absorbed must have exceeded the fracture energy of the PMMA samples “A” and “B”. As a result of this process, the samples broke into pieces.

Since the mechanical properties of PMMA are strongly rate sensitive, failure behavior changes from ductile to brittle as strain rate increases. At increasing strain rate, the periodic time gap between the energy accumulation and release becomes progressively smaller. This leaves the PMMA samples with very little time to relax and readjust the localized huge strain development through its own chain mobility. As a result of this process, cracks are initiated rather quickly into the PMMA samples “A” and “B”. However, only initiation of cracks does not ensure failure. The failure of PMMA “A” and “B” happens when the strain rate reaches a certain critical value (e.g., $\sim 7.69 \times 10^2 \text{ s}^{-1}$) that leads to the rapid and uneven extension of the existing cracks until the specimen fractures [20]. This is possibly why the PMMA samples “A” and “B” did not necessarily fail at the highest strain rates achieved during the present SHPB experiments.

The scanning electron microscope (SEM) photomicrographs of the fracture surfaces of PMMA “A” sample, collected after the SHPB tests, are shown in Fig. 6a, b. It is evident from Fig. 6a that some local melting of the PMMA chains have had taken place during the propagation of the shock pulse across the sample during the high strain rate SHPB tests. Similarly, from the features displayed in Fig. 6b, the possibility of a highly localized shear deformation cannot be totally ruled out.

It is well known that an increase of strain rate decreases the molecular mobility of the polymer chains by making the chains stiffer [4, 24]. Many molecular theories have been proposed [4, 24] to predict the yield stress of amorphous polymers undergoing compressive/tensile loading. These models have taken into account the yield behavior of PMMA as a thermally activated process. Subsequently, attempts were made to decouple the individual influence of strain rate from the individual influence of temperature in the entire failure mechanisms of PMMA [24]. Recent efforts [25] have also showed that relaxation rates increased substantially, when the PMMA specimens were stretched beyond the yield point. It was claimed that, such an observation implied the existence of chain mobility in the unstressed surface of PMMA that got enhanced around surface depressions, following the onset of local plasticity.

Yielding of the amorphous polymers under compressive load involves movement of the polymer chains in a cooperative fashion to accommodate deformation within the activation volume that gets generated during the high strain rate loading process [3, 4]. Successful attempts were also made very recently [4] to accommodate the temperature dependence of both effective stress and the characteristic strain rate into this general mathematical formalism to cover a wide range of strain rates and stresses. This effort confirmed that there is a strong correlation between the yielding

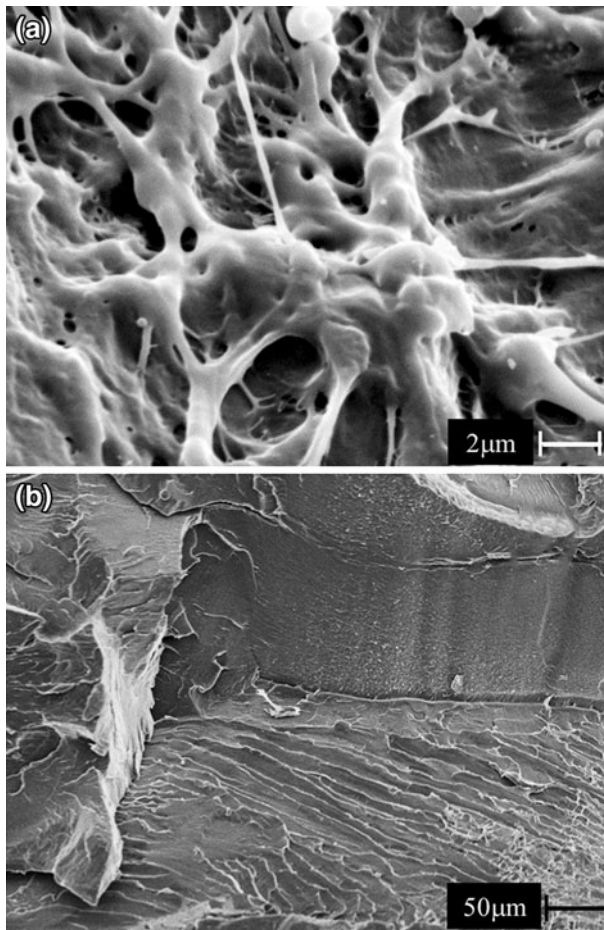


Fig. 6 The SEM photomicrographs of fracture surfaces of PMMA “A” sample after failure suggesting localized **a** melting and **b** shear deformation

process and segmental mobility of the β -relaxation process in amorphous polymers such as PMMA [4].

It is well known that PMMA deforms initially by bulk plastic flow, followed by initiation of parallel and perpendicular cracks and finally, by both shear damage growth as well as random cracking [13]. If it is assumed that the temperature generated at the crack tip is due to release of the elastic strain energy stored in the PMMA sample during the high strain rate experiments then the samples which suffered the most catastrophic failure [“A” and “B”] should have suffered mostly from temperatures at the crack tips.

Although no attempt was made in the present experiments to measure the temperature of the PMMA samples during the high strain rate loading processes, but the maximum temperature that could be generated at the crack tip has been estimated to be ~ 530 °C [13]. The typical decomposition temperature for PMMA

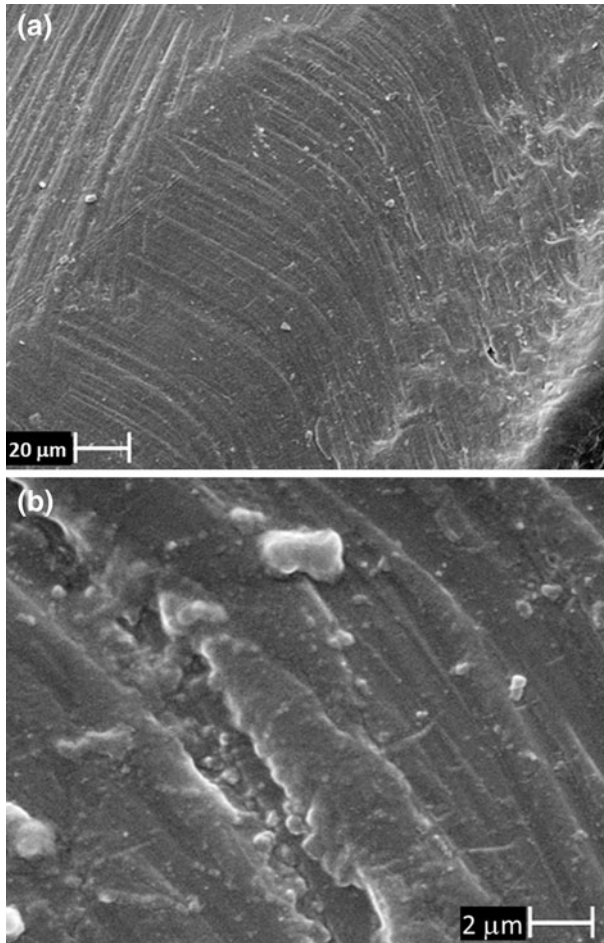


Fig. 7 The SEM pictures **a**, **b** of the post-SHPB test deformed surfaces of the PMMA samples “C”, showing the possibility of localized rise in temperature during the SHPB experiments

is ~ 360 °C, while the softening temperature for the present PMMA samples is even lower e.g., ~ 102 °C (Table 1). Therefore, local decomposition possibility cannot be ruled out for PMMA “A”. The SEM photomicrographs shown in Fig. 6a indeed provides very strong indirect support in favor of this conjecture. Similar features were also found in SEM examinations for the PMMA sample “B”, but were not included in the present communication for the sake of brevity.

When the specimen deformed without fracture, as was the case with the PMMA samples “C” and “D”, the energy absorbed by it must have been transformed into elastic strain energy. When this strain energy is released, similar to the case of “A” and “B”, it would lead to localized heat generation at the tip of the existing cracks in “C” and “D”. But the amount of heat generated in “C” and “D” could be lesser than those generated in “A” and “B”, since the strain rates in “C” and “D” were much lesser (Fig. 3) than those of “A” and “B”.

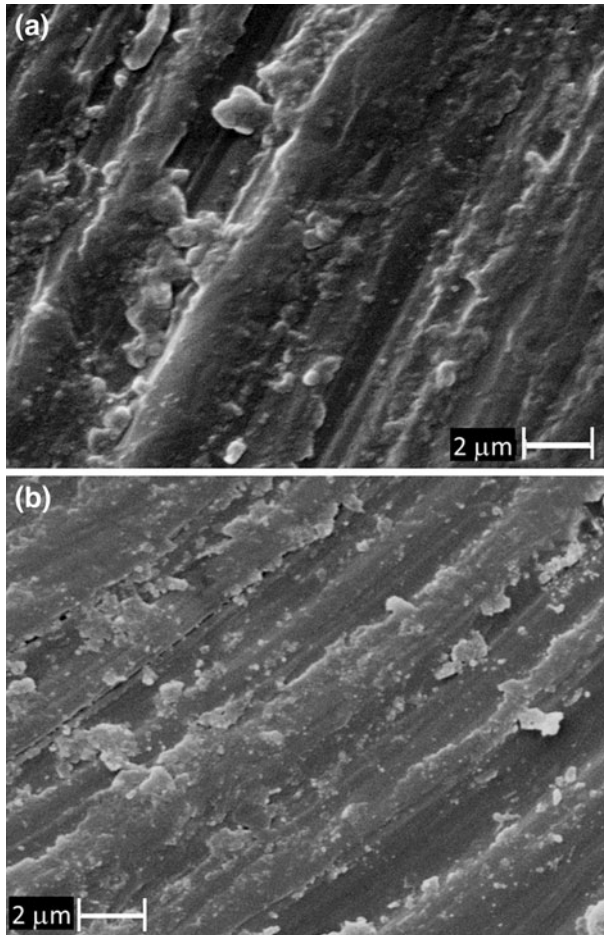


Fig. 8 The SEM images **a**, **b** of the post-SHPB test deformed surfaces of the PMMA sample “C”, suggesting the possibility of strain softening at the peak stress attained during the SHPB experiments

But, even then adequate local rise in temperature is possible [13, 21]. Given the fact that the present PMMA had a relatively lower softening temperature of 102 °C (Table 1), the effect of localized adiabatic heating on the strain softening cannot be neglected [23].

If such a situation prevailed in the PMMA samples “C” and “D” it would lead to a deformed microstructure without going to the extent of melting. The representative SEM photomicrographs of the surfaces of unbroken PMMA specimen “C” collected after the SHPB tests are shown in Fig. 7a, b. It appears from these two photomicrographs that the microstructure is deformed, which might have had happened, due to localized rise in temperature, as suggested above.

Similarly, the SEM photomicrographs depicted in Fig. 8a, b appear to suggest in favor of strain softening that had happened at the peak stress for the PMMA sample

“C”. Similar characteristic evidences were also found during SEM examinations of the deformed surfaces of the PMMA sample “D”, but has been deliberately kept outside the present communication for the sake of brevity.

According to the Ree–Eyring theory [26], the temperature and strain rate dependencies of the yield behavior are related to the specific degrees of freedom of the chains for a given polymer. When a given degree of freedom becomes suddenly restricted at high strain rate, the corresponding process begins to contribute to the overall resistance of the material against deformation. Thus, based on the present experimental evidences and literature data [22] it may be suggested that a fraction of the energy spent in localized plastic deformation was converted to heat. As a consequence, the PMMA samples “C” and “D” might have had experienced some thermal softening that could have led to deformations without fracture at the strain rates of $\sim 4.75 \times 10^2$ to $6.75 \times 10^2 \text{ s}^{-1}$, (Fig. 3).

Conclusions

The major conclusions of the present work are:

- (a) The maximum compressive yield strength of the present PMMA samples increased from about 281–351 MPa (i.e., by $\sim 25\%$) with the corresponding enhancement in strain rates e.g., from $\sim 4.75 \times 10^2$ to $9.31 \times 10^2 \text{ s}^{-1}$.
- (b) The failure processes of the current PMMA samples had initiated beyond a critical value (e.g., $\sim 7.69 \times 10^2 \text{ s}^{-1}$) of strain rate.
- (c) The experimental data and existing knowledgebase suggested that for the present PMMA samples undergoing deformation followed by fracture in the SHPB experiments, two mechanisms might have had occurred either independent of or simultaneously with each other. These are proposed to be, the thermal decomposition due to localized rise in temperature during high strain rate impact; and the localized shear flow due to high stress concentration at existing crack tips.
- (d) In addition, it is suggested that the presence or absence of strain induced localized and/or global softening of the material’s microstructure have a strong bearing on the high strain rate dynamic behavior of PMMA samples undergoing deformation with or without brittle fracture.

Acknowledgments The authors thank Mr. Kamal Dasgupta, Director, CSIR-CGCRI for his kind permission to publish this paper. The authors gratefully acknowledge that the present SHPB experiments were carried out at IIT Kanpur under the supervision of Prof P. Venkitanarayanan. The financial support of the Council of Scientific and Industrial Research (CSIR), Govt. of India (Project no. NWP 0029) in carrying out the present research work is gratefully acknowledged. The authors also appreciate the kind of encouragements received from Prof. I. Manna, Director, IIT Kanpur and Dr. S. K. Biswas, Chief Scientist, CSIR-CGCRI.

References

1. Roetling J (1965) Yield stress behavior of polymethylmethacrylate. *Polymer* 6:311–317

2. Moy P, Gunnarsson CA, Weerasooriya T, Chen W (2011) Stress–strain response of PMMA as a function of strain-rate and temperature. *Conf Proc Soc Exp Mech Ser* 99:125–133
3. Richeton J, Ahzi S, Daridon L, Remond Y (2005) A formulation of the cooperative model for the yield stress of amorphous polymers for a wide range of strain rates and temperatures. *Polymer* 46:6035–6043
4. Richeton J, Ahzi S, Vecchio KS, Jiang FC, Adharapurapu RR (2006) Influence of temperature and strain rate on the mechanical behavior of three amorphous polymers: characterization and modelling of the compressive yield stress. *Int J Solid Struct* 43:2318–2335
5. Wu H, Ma G, Xia Y (2004) Experimental study of tensile properties of PMMA at intermediate strain rate. *Mat Lett* 58:3681–3685
6. Chen W, Lu F, Cheng M (2002) Tension and compression tests of two polymers under quasi-static and dynamic loading. *Polym Test* 21:113–121
7. Li Z, Lambros J (2001) Strain rate effect on the thermomechanical behavior of polymers. *Int J Solid Struct* 38:3549–3562
8. Blumenthal WR, Cady CM, Lopez MF, Gray GT III, Idar DJ (2001) Influence of temperature and strain rate on the compressive behavior of PMMA and polycarbonate polymers. *AIP Conf Proc* 620:665–668
9. Moy P, Weerasooriya T, Chen W, Hsieh A (2003) Dynamic stress–strain response and failure behavior of PMMA. *IMECE2003-43371*: 105–109
10. Chou SC, Robertson KD, Rainey JH (1973) The effect of strain rate and heat developed during deformation on the stress–strain curve of plastic. *Exp Mech* 13(10):422–432
11. Walley SM, Field JE, Pope PH, Stafford NA (1989) A study of the rapid deformation behavior of a range of polymers. *Phil Trans R Soc Lond A* 328(1597):1–33
12. Arruda Ellen M, Boyce Mary C, Jayachandran R (1995) Effects of strain rate, temperature and thermomechanical coupling on the finite strain deformation of glassy polymers. *Mech Mater* 19(2–3):193–212
13. Swallowe GM, Field JE, Horn LA (1986) Measurements of transient high temperatures during the deformation of polymers. *J Mater Sci* 21:4089–4096
14. Swallowe GM, Lee SF (2003) A study of the mechanical properties of PMMA and PS at strain rates of 10^{-4} to 10^3 over the temperature range 293–363 K. *J Phys IV France* 110:33–38
15. Woldesenbet E, Vinson Jack R (1999) Specimen geometry effects on high-strain-rate testing of graphite/epoxy composites. *AIAA J* 37(9):1102–1106
16. Gray GT III, Blumenthal WR (2000) Mechanical testing and evaluation. *ASM Handb* 8:488–496
17. Cady CM, Blumenthal WR, Gray GT III, Idar DJ (2003) Determination of constitutive response of polymeric materials as a function of temperature and strain rate. *J Phys IV France* 110:27–32
18. Liu Q, Subhash G (2006) Characterization of viscoelastic properties of polymer bar using iterative deconvolution in the time domain. *Mech Mater* 38(12):1105–1117
19. Naik NK, Rao KV, Veerraju Ch, Ravikumar G (2010) Stress–strain behavior of composites under high strain rate compression along thickness direction: effect of loading condition. *Mater Design* 31:396–401
20. Wu H, Ma G, Xia Y (2004) Experimental study of tensile properties of PMMA at intermediate strain rate. *Mater Lett* 58:3681–3685
21. Yokoyama T, Nakai K (2010) Determination of high strain-rate compressive stress–strain loops of selected polymers. *Appl Mech Mater* 24–25:349–355
22. Mulliken AD, Boyce MC (2006) Mechanics of the rate-dependent elastic-plastic deformation of glassy polymers from low to high strain rates. *Int J Solid Struct* 43:1331–1356
23. Nasraoui M, Forquin P, Siad L, Rusinek A (2012) Influence of strain rate, temperature and adiabatic heating on the mechanical behavior of poly-methyl-methacrylate: experimental and modelling analyses. *Mat Design* 37:500–509
24. Fuller KNG, Fox PG, Field JE (1975) The temperature rise at the tip of fast-moving cracks in glassy polymers. *Proc R Soc Lond A* 341:537–557
25. Bucknall CB (2012) Role of surface chain mobility in crazing. *Polymer* 53:4778–4786
26. Ree T, Eyring H (1955) Theory of non-Newtonian flow. I. Solid plastic system. *J Appl Phys* 26(7):793–800